On the KBSM of links in lens spaces

Boštjan Gabrovšek, Enrico Manfredi

June 4, 2015

Abstract

In this paper the properties of the Kauffman bracket skein module of $L(p,q)$ are investigated. Links in lens spaces are represented both through band and disk diagrams. The possibility to transform between the diagrams enables us to compute the Kauffman bracket skein module on an interesting class of examples consisting of inequivalent links with equivalent lifts in the 3-sphere. The computation show that the Kauffman bracket skein module is an essential invariant, that is, it may take different values on links with equivalent lifts. We also show how the invariant is related to the Kauffman bracket of the lift in the 3-sphere.

Mathematics Subject Classification 2010: Primary 57M25, 57M27; Secondary 57M10.

Keywords: knots/links, lens spaces, lift, skein module, Kauffman bracket.

1 Introduction

Skein modules play an important role in geometric topology since they capture essential information about the geometry of 3-manifolds. For instance, they reflect the interaction between embedded 1-dimensional and embedded 2-dimensional submanifolds, in particular, the existence of an embedded non-separating surface produces torsion in the module [P].

Our focus will be the Kauffman bracket skein module (KBSM) of links in lens spaces $L(p,q)$. This module is of particul interest since it is a non-trivially finitely generated skein module. The motivation for studying links in lens spaces can also be justified in recent applications to biology [BM] and physics [S].

As for the paper itself, it represents a merge of the theses of the first author [Ga] and second author [M1].

When studying knots in lens spaces, we can immediately notice that several different knot representations are scattered throughout literature. For example, band diagrams were originally used to calculate the KBSM of $L(p, q)$ [HP]. Closely related punctured disk diagrams were used to tabulate knots in $L(p, q)$ [Ga]. It was recently shown in [CMM] that it is possible to generalize Drobotukhina's disk diagram for the projective space to the case of $L(p, q)$. Disk diagrams, which follow the algebraic description of $L(p, q)$ more closely, allow us to construct a straightforward Wirtinger-type presentation of the link group [CMM] and allow us to study lifts of knots in $L(p, q)$ to the cyclic cover S^3 [M2].

In order to better understand different representations of knots in $L(p, q)$, we explicitly show in Section 2 how to transform one diagram to the other.

In section 3 we show how to construct the lift of a link in $L(p, q)$ to a link in S^3 using band diagrams. In addition, we show that the KBSM is an essential invariant, that is to say, the KBSM may have different values on links with equivalent lifts. This, on the one hand, provides another evidence that the links considered in [M2], with equivalent lift, are actually distinct, and on the other hand, it shows that the KBSM is a genuine $L(p, q)$ link invariant that cannot be simply derived from an S^3 link invariant of the lift.

At last, in Section 4, following an idea of Chbili [C] about the Jones polynomial of freely periodic knots, we show the connection between the KBSM of a link in a lens space and the KBSM of its lift in $\mathbf{S}^3$

2 Different representations of links in lens spaces

The aim of this section is to recall the possible representations of links in lens spaces, namely, the disk diagram of [CMM], the band diagram of [HP], and the closely related punctured disk diagram of [Ga]. We show how to switch from one representation to the other.

Basic definitions Let $L(p, q)$ denote the lens space obtained by a p/q rational surgery on the unknot in the 3-sphere $\mathbf{S}^3$. Here p and q are coprime integers satisfying $0 \leq q < p$.

A n-component link L in a $L(p, q)$ is the embedding of n copies of $\mathbf{S}^1$ to $L(p, q)$. A link $L \subset L(p, q)$ is *trivial* if its components bound n pairwise disjoint 2-disks

in $L(p, q)$. Two links $L, L' \subset L(p, q)$ are called *equivalent* if there exists a smooth ambient isotopy between them.

Band diagrams and punctured disk diagrams Let L be a link in $L(p, q)$ described by p/q-rational surgery over the unknot U as before. Such a link can be presented as a mixed link $L \cup U \subset \mathbf{S}^3$ [DL]. Let x be a point of U and send it to ∞ in order to describe $\mathbf{S}^3$ with the one-point compactification of $\mathbb{R}^3$. Let (x_1, x_2, x_3) be the coordinates of $\mathbb{R}^3$. Assume that U is described by the x_3 axis. Consider the orthogonal projection $\mathbf{p}$ of $L \cup U$ on the $x_1 x_2$ plane. Up to small isotopies of L, we can assume that this projection is *regular*, that is:

1) the projection of L contains no cusps;

2) all auto-intersections of $\mathbf{p}(L)$ are transversal;

3) the set of multiple points is a finite set of double points.

The *punctured disk diagram* of $L \subset L(p, q)$ is a regular projection of $L \cup U$, where U is projected to a "dot" (see Figure 1). If we just consider the space $\mathbf{S}^3 \setminus U$ without the Dehn filling, a dotted diagram can also describe a link in the solid torus [GM].

A *band diagram* for a link $L \subset L(p, q)$ is obtained from a punctured disk diagram through the construction depicted in Figure 1: cut the punctured disk diagram along a line orthogonal to the boundary and avoiding the crossings of L, then deform the annulus into a rectangle. This operation can easily be reversed.
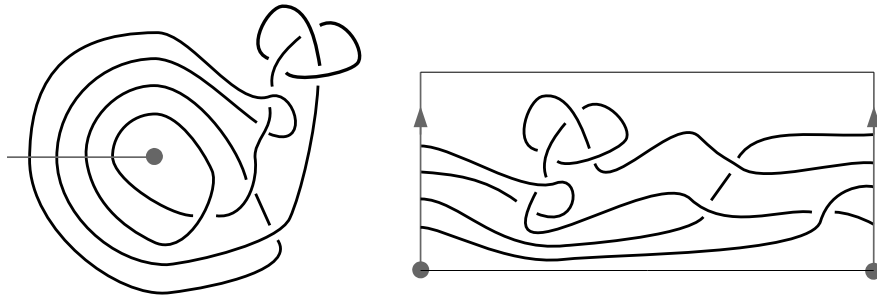

Figure 1: An example of punctured disk diagram and band diagram for a link in $L(p, q)$.

Reidemeister moves for punctured disk diagrams Punctured disk diagrams for $L(p, q)$ are accompanied by the three classical Reidemeister moves and an additional slide move SL that arises from the p/q-surgery (see [HP, Ga] for details).
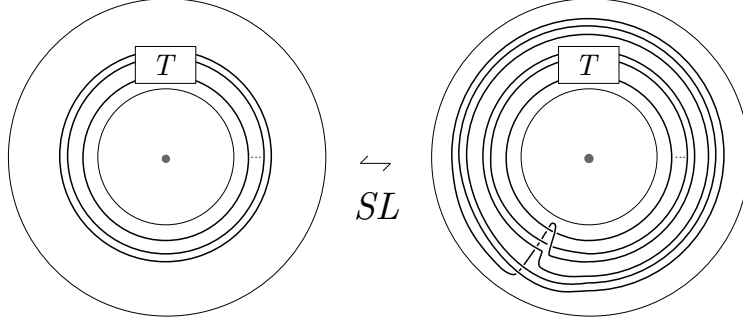

Figure 2: SL move on punctured disk diagram for the case $L(3, 1)$.

The lens model for lens spaces A lens space may be defined also by the following model: considering the 3-dimensional ball B^3 and let E_+ and E_- be respectively the upper and the lower closed hemisphere of ∂B^3. The equatorial disk B_0^2 is defined as the intersection of the plane $x_3 = 0$ with B^3. Label with N and S respectively the north pole $(0, 0, 1)$ and the south pole $(0, 0, -1)$ of B^3. Let $g_{p,q} \colon E_+ \to E_+$ be the counterclockwise rotation of $2\pi q/p$ radians around the x_3-axis and let $f_3 \colon E_+ \to E_-$ be the reflection with respect to the plane $x_3 = 0$ (Figure 3).

The *lens space* $L(p, q)$ is the quotient of B^3 by the equivalence relation on ∂B^3 which identifies $x \in E_+$ with $f_3 \circ g_{p,q}(x) \in E_-$. The quotient map is denoted by $F \colon B^3 \to L(p, q) = B^3/\sim$. Note that on the equator $\partial B_0^2 = E_+ \cap E_-$ each equivalence class contains p points, instead of the two points contained in the equivalence classes outside the equator. The first example is $L(1, 0) \cong \mathbf{S}^3$ and the second example is $L(2, 1) \cong \mathbb{RP}^3$, where the construction gives the usual model of the projective space with opposite points on ∂B^3 identified.

The disk diagram Since we are not interested in the case of $\mathbf{S}^3$, we assume $p > 1$. Intuitively, a *disk diagrams* of a link L in $L(p, q)$, represented by the lens model, is a regular projection of $F^{-1}(L)$ onto the equatorial disk of B^3, with the resolution of double points with overpasses and underpasses. In order to have a comprehensible diagram, we label with $+1, \ldots, +t$ the endpoints of the projection of the link coming from the upper hemisphere, and with $-1, \ldots, -t$ the endpoints coming from the
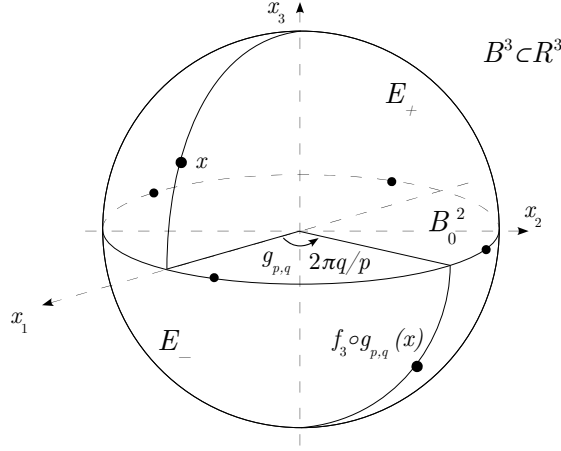
4

Figure 3: Representation of $L(p, q)$.

lower hemisphere, respecting the rule $+i \sim -i$ (see [CMM] for more details). An example is shown in Figure 4.
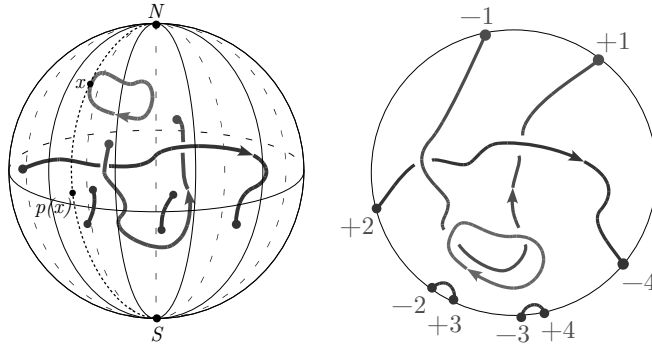

Figure 4: A link in $L(9, 1)$ and its corresponding disk diagram.

Reidemeister moves for disk diagrams   Two disk diagrams of links in lens space represent equivalent links if and only if they are connected by a finite sequence of the Reidemeister moves illustrated in Figure 5 [CMM].

Standard form of the disk diagram   A disk diagram is defined *standard* if the labels on its boundary points, read according to the orientation on ∂B_0^2, are $+1, \ldots, +t, -1, \ldots, -t$.
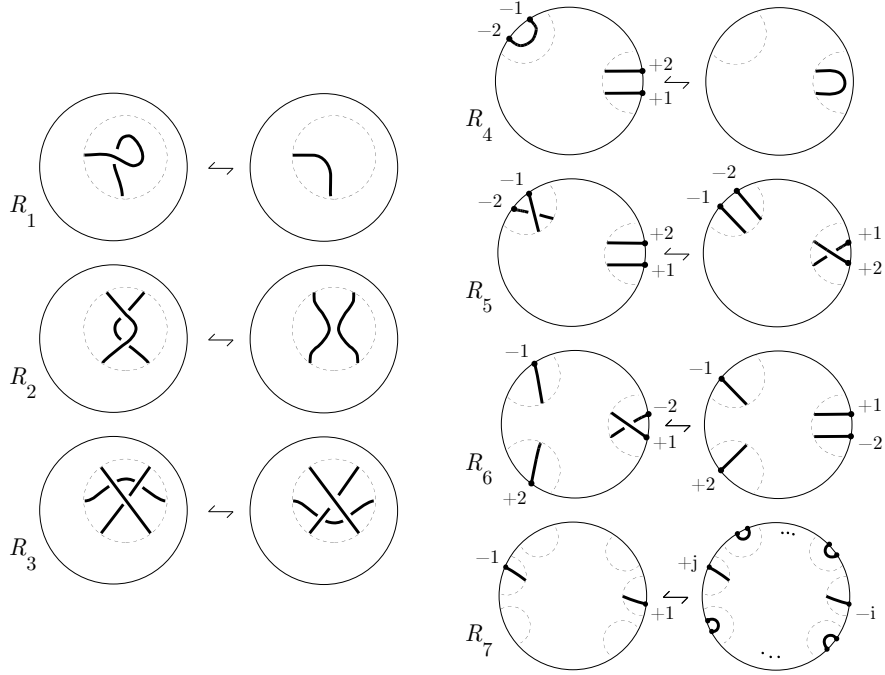
Figure 5: Generalized Reidemeister moves.

Proposition 1. [M2] *Every disk diagram can be reduced to a standard disk diagram using small isotopies: if $p = 2$, the signs of its boundary points can be exchanged; if $p > 2$, a finite sequence of R_6 moves can be applied in order to bring all positive boundary points aside.*

Equivalence between link diagrams At this point we describe a geometric transformation between disk and punctured disk diagrams. Note that the transformation between punctured disk diagrams and band diagrams has already been described in the previous paragraphs.

Let B_t be the braid group on t letters and let $\sigma_1, \ldots, \sigma_{t-1}$ be the Artin generators of B_t. Consider the Garside braid Δ_t on t strands defined by

$$(\sigma_{t-1}\sigma_{t-2}\cdots\sigma_1)(\sigma_{t-1}\sigma_{t-2}\cdots\sigma_2)\cdots(\sigma_{t-1}),$$

and illustrated in Figure 6. Note that Δ_t represents a positive half-twist of all the braid strands. The braid Δ_t^2 belongs to the center of the braid group, i.e. it commutes with every braid. Moreover, Δ_t^{-1} can be written, after some braid operations, as

$$(\sigma_{t-1}^{-1}\sigma_{t-2}^{-1}\cdots\sigma_1^{-1})(\sigma_{t-1}^{-1}\sigma_{t-2}^{-1}\cdots\sigma_2^{-1})\cdots(\sigma_{t-1}^{-1}).$$
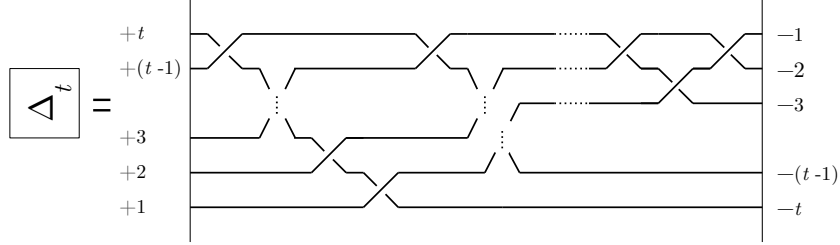
Figure 6: The braid Δ_t.

The following Proposition explains how to transform a band diagram into a standard disk diagram.

Proposition 2. *Let L be a link in $L(p,q)$ assigned via a band diagram B_L. A standard disk diagram D_L representing L can be obtained by the construction depicted in Figure 7.*
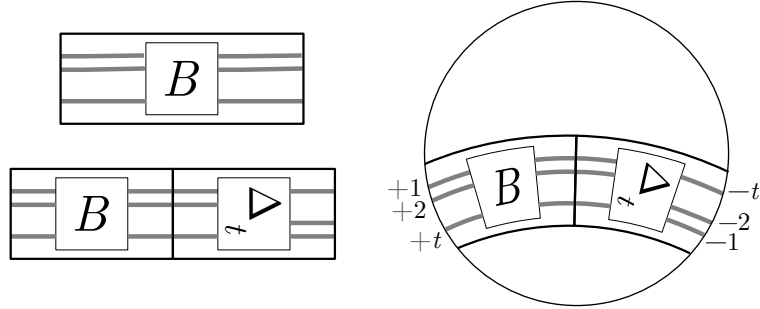

Figure 7: From band diagram B_L to disk diagram D_L in $L(p,q)$.

Consider the band diagram B_L, the rectangle has two opposite identified sides, with t points on each of them; add to the right side of the band diagram the braid Δ_t, then put the resulting band inside a disk, with the opposite sides of the new rectangle on the boundary of the disk. Add the indexation $+1, +2, \ldots, +t$ on the points of the left side of the rectangle and $-1, -2, \ldots, -t$ on the other boundary points: the result is the desired disk diagram D_L.

Proof. The band diagram may be seen as the result of a genus one Heegaard splitting of $L(p,q)$, where the link is contained inside one of the two solid tori and is regularly projected on the annulus which has as a boundary of q longitudes of the solid torus.

Following the geometric description of the equivalence between the Heegaard splitting model and the lens model of the lens spaces, depicted for the particular case of $L(5,2)$ in Figure 8, we can put the band diagram in one solid torus as depicted in Figure 9,
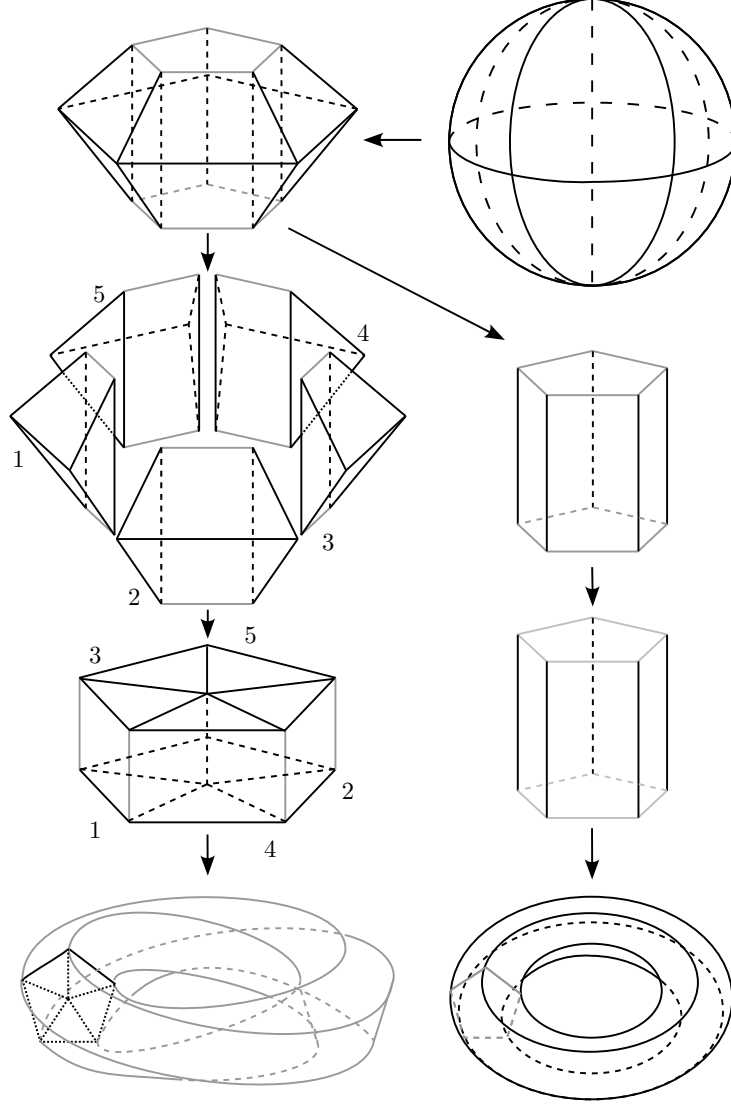

Figure 8: From the lens model to Heegaard splitting.

then put the solid torus inside the lens model of the lens space, and project the band diagram onto the equatorial disk. During this operation, we have a twist, described by Δ_t. Finally, adding the labels to the boundary points, we get the desired disk diagram D_L. □
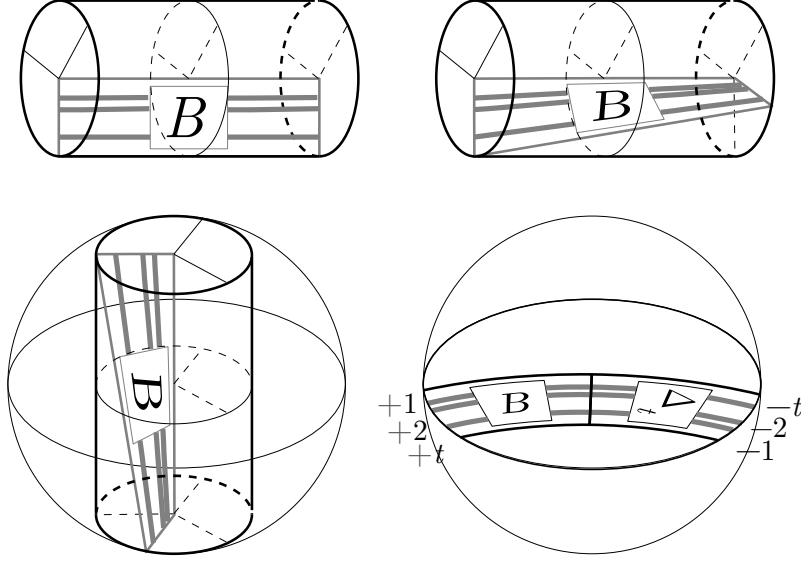
Figure 9: From the Heegaard splitting to the lens model of $L(p, q)$.

On the other hand, we can recover the band diagram of a link from the disk diagram.

Proposition 3. *Let L be a link in $L(p, q)$, described by a disk diagram. Let D_L be the standard disk diagram obtained from Proposition 1. A band diagram B_L for L is constructed using the geometric algorithm described in Figure 10.*
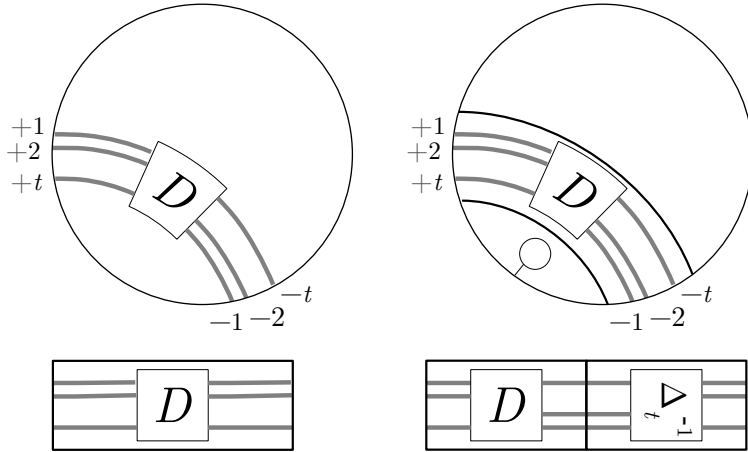

Figure 10: From disk diagram D_L to band diagram B_L in $L(p, q)$.

9

Consider the disk diagram D_L and open the disk on the right of the $+1$ point, as in Figure 10; this way a rectangle is obtained, with identified points only on the left and right sides, then add the braid Δ_t^{-1} on the right side and this is the desired band diagram for L.

Proof. It is exactly the converse geometric construction of the proof of Proposition 2. □

The intuitive correspondence between the Reidemeister moves on the disk diagrams and the band diagrams are represented in Table 2.

Disk diagram	Band diagram
R_1	R_1
R_2	R_2
R_3	R_3
R_4	isotopy of an arc
R_5	isotopy of a crossing
R_6	not allowed on standard diagram
R_7	SL

3 The KBSM of links in $L(p,q)$ is an essential invariant

In this section we provide examples of different links with equivalent lifts of [M2] to show that the KBSM is an essential invariant, that is to say, it may distinguish links with equivalent lifts.

KBSM of links in lens spaces via punctured disk diagrams The KBSM of a 3-manifold M, denoted by $S_{2,\infty}(M)$, is defined in the following way. Take an unoriented framed link $L \subset M$ and let $\mathcal{L}_{fr}$ be the set of ambient isotopy classes of unoriented framed links in M, where we also add the empty knot $\emptyset$. Let $L^{(n)}$ denote the framed link obtained by $L \subset \mathcal{L}_{fr}$ by adding n full right-handed twists to the framing. Let $R = \mathbb{Z}[A^{\pm 1}]$ be the ring of Laurent polynomials in variable A. Define $\mathcal{S}_{fr}$ to be the submodule of $R\mathcal{L}_{fr}$ generated by the skein relations $L - AL_0 - A^{-1}L_\infty$ and $L^{(1)} + A^3L$, where L_0 and L_∞ denote the links obtained by the resolutions of one crossing of L as Figure 11 shows.
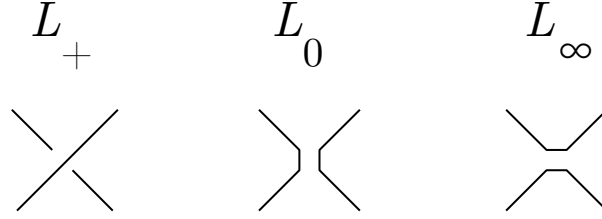
$$L_+ \qquad L_0 \qquad L_\infty$$

Figure 11: Resolution of a crossing of L.

The *Kauffman bracket skein module* is the quotient $S_{2,\infty}(L(p,q)) = R\mathcal{L}_{fr}/\mathcal{S}_{fr}$.

In order to understand the skein module for a particular 3-manifold M, we have to present a basis of the module and understand the torsion (if it exists).

We use the representation of links in lens space given by a punctured disk diagram. These diagrams are useful also to represent links in the solid torus (see Section 2). Let x_0 denote the local unknot in the solid torus and x_i denote the link with i components described in Figure 12.
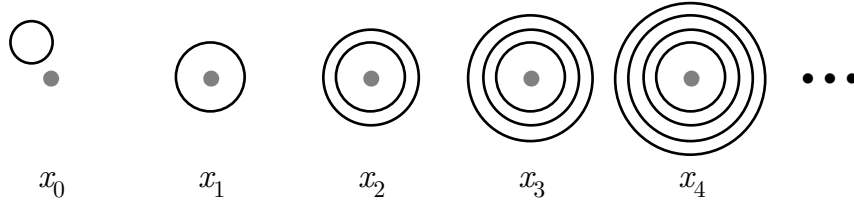

Figure 12: KBSM basis for the punctured disk diagram.

Proposition 4. [T, Corollary 2] *The KBSM of the solid torus is freely generated by the set $\{x_i\}_{i\in\mathbb{N}}$.*

The following proposition has been presented in [HP]:

Proposition 5. [HP, Theorem 4] *For $p \geq 1$ the KBSM of $L(p,q)$ is freely generated by $x_0, x_1, \ldots, x_{\lfloor p/2 \rfloor}$, where $\lfloor r \rfloor$ denotes the integer part of r.*

Remark 6. The computation of the Kauffman bracket of a link in $L(p,q)$ described by a punctured disk diagram is performed using the following algorithm: simplify all the crossings with the skein relation and once you are left only with the diagrams of Figure 12, substitute each x_i for all $i > \lfloor p/2 \rfloor$ with a suitable linear combination of

the basis $x_0, x_1, \ldots, x_{\lfloor p/2 \rfloor}$. The formula for x_i, $i > \lfloor p/2 \rfloor$, can be found by considering x_{i-p} (or x_{p-i} if $i - p < 0$), applying an SL move and resolving the crossings with the skein relation. In the case where the winding number $w(L)$ of the link in the lens space is lower than $\lfloor p/2 \rfloor$, the KBSM of links in lens spaces coincide with the one in the solid torus.

As a consequence, the KBSM of a knot in $L(p, q)$ can be recovered from the KBSM of the corresponding knot in the solid torus T under the standard inclusion of $T \subset L(p, q)$. Through this method [Ga] provided the KBSM-s of knots in $L(p, q)$ up to 5 crossings.

Lift of links in lens spaces Following [M2] we are able to construct a diagram of the lift of a link in $L(p, q)$ starting from a disk diagram. Using Proposition 3 we are able to construct a similar diagram of the lift starting from a band diagram, as shown in the following proposition.

Proposition 7. *Let L be a link in the lens space $L(p, q)$ and let B be a band diagram for L with t boundary points; then a diagram for the lift $\widetilde{L} \subset \mathbf{S}^3$ can be found by juxtaposing p copies of B and closing them with the braid Δ_t^{2q} (see Figure 13).*
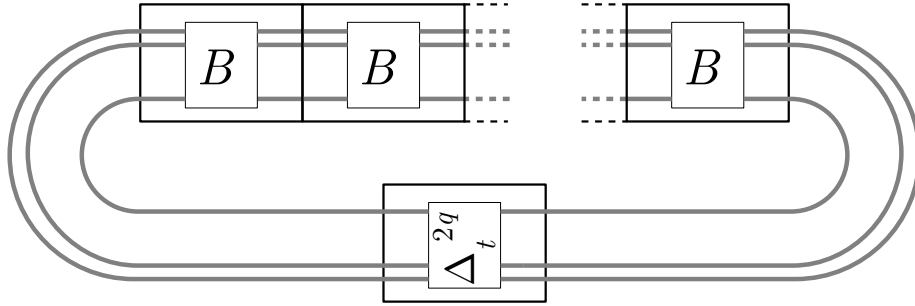

Figure 13: Diagram of the lift of a link in lens spaces from its band diagram.

Proof. Consider the planar diagram of the lift of [M2, Theorem 3] and convert the standard disk diagram D_L plus the braid Δ_t^{-1} to the equivalent band diagram B_L. This gives exactly the diagram for $\widetilde{L}$ illustrated in Figure 13. $\qquad\square$

Remark 8. The lift in $\mathbf{S}^3$ of a link $L \subset L(p, q)$ is exactly a (p, q)-*lens link* in $\mathbf{S}^3$, according to [Ch4]. Precisely, the n-tangle T that Chbili uses in his construction is the band diagram B_L for L. In the same paper he makes explicit that the lift is a freely periodic link in $\mathbf{S}^3$.

Essential invariants It is clear that every link invariant in $\mathbf{S}^3$ induces a link invariant in $L(p,q)$ if the first invariant is computed on the lift. On the contrary, it is important to know if an link invariant for $L(p,q)$ is a real $L(p,q)$ invariant or just an S^3 invariant in disguise. If an $L(p,q)$ invariant can take different values on two links with equivalent lifts, we call such an invariant *essential*.

Inequivalent links with equivalent lifts are perfect candidates to check whether an invariant I of links in lens spaces is essential: find two inequivalent knots K_1 and K_2 with equivalent lifts such that $I(K_1) \neq I(K_2)$.

KBSM is an essential invariant In [M2] are shown several examples which consist of different links with equivalent lifts. By applying Proposition 3 we can transform the disk diagram of the knots into band diagrams and consequently compute the Kauffman bracket for them. The result of the computations shows us that the KBSM is an essential invariant.

Example 9. In Figure 14 are represented the punctured disk diagrams of the knots K_1 and K_2 in $L\left(p, \frac{p\pm 1}{2}\right)$. When $p > 3$ and odd, the two knots are not isotopic and they both lift to the unknot in $\mathbf{S}^3$, as shown in [M2, Example 9]. It holds that
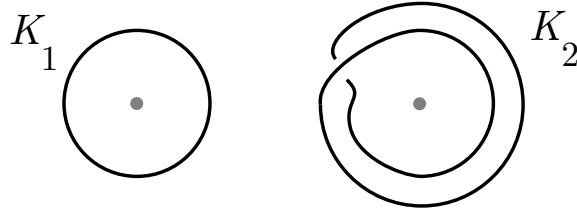

Figure 14: Punctured disk diagrams K_1 and K_2 in $L\left(p, \frac{p\pm 1}{2}\right)$.

$\text{KBSM}(K_1) = x_1$ and $\text{KBSM}(K_2) = Ax_2 + A^{-1}x_0$.

Example 10. The two links L_A and L_B in $L(4,1)$, represented by the punctured disk diagrams of Figure 15, are not isotopic since they have a different number of components, but they both lift to the Hopf link, as shown in [M2, Example 10]. It holds that $\text{KBSM}(L_A) = Ax_2 + A^{-1}x_0$ and $\text{KBSM}(L_B) = x_2$.

Example 11. Consider the two links $A_{2,2}$ and $B_{2,2}$ in $L(4,1)$, represented by the punctured disk diagrams illustrated in Figure 16. Their punctured disk diagram are found according to Proposition 3, starting from [M2, Example 11]. The links are not
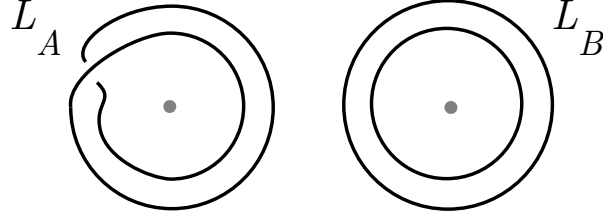
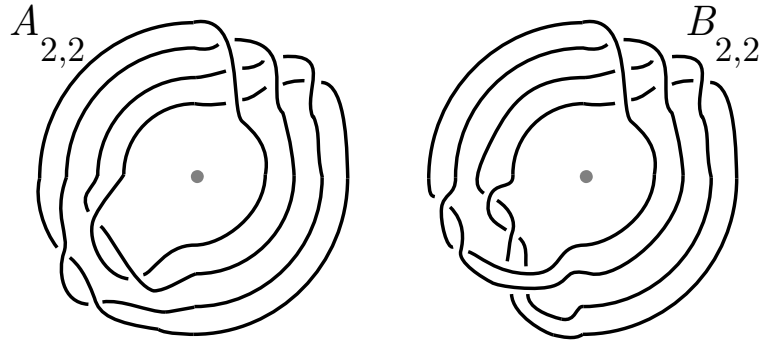Figure 15: Punctured disk diagrams for L_A and L_B in $L(4,1)$.

Figure 16: Punctured disk diagrams for $A_{2,2}$ and $B_{2,2}$ in $L(4,1)$.

isotopic as they have different Alexander polynomials, but they have equivalent lifts.

Their KBSM-s are again different:

$$\text{KBSM}(A_{2,2}) = (3A^{14} + A^{10} - 2A^8 - A^6 - 1)x_2+$$
$$+ (-A^{20} + A^{12} - A^6 - A^{-2} + A^{-4} - A^{-8} + A^{-12} - A^{-16})x_0$$

$$\text{KBSM}(B_{2,2}) = (3A^{12} + A^8 - 2A^6 + 2A^2 + 2 + 4A^{-2} + 2A^{-4})x_2+$$
$$+ (-A^{18} + A^{10} - A^4 + 1 + 3A^{-4} - A^{-6} + 5A^{-8} - 3A^{-10} + 4A^{-12} - 3A^{-14} - A^{-18})x_0.$$

4   KBSM vs KB of the lift

In this section we show a relation between the KBSM of a link L in $L(p,q)$ and the Kauffman bracket of the lift.

Let B be a punctured disk diagram of L (or equivalently, a band diagram, as Section 2 shows). We can consider the punctured disk diagram as a diagram of L

in the solid torus, and compute the KBSM of L inside the solid torus according to Proposition 4. Let $\delta = -A^{-2} - A^2$. A substitution of x_0 with 1 and x_i, $i > 0$, with δ^{i-1} yields the usual Kauffman bracket of links in $\mathbf{S}^3 = L(1,0)$ which we denote by $\langle L \rangle$.

Let t denote half of the number of boundary points of B. Following Remark 8 we can describe B as a t-tangle, and we can describe the lift of the link as a sum of t-tangles: $B^p \Delta_t^{2q}$. The closure of a t-tangle $\widehat{B}$ is a link in $\mathbf{S}^3$ and it coincides with the link in $\mathbf{S}^3 = L(1,0)$ represented by the band diagram B. In the case where the winding number $w(L)$ of the link in the lens space is lower than $\lfloor p/2 \rfloor$, the statement is true also for the KBSM of the link in the lens space. Let Id_t denote the trivial braid on t strands, or equivalently, the trivial t-tangle. The link $\widehat{Id_k}$ is the unlink with k components.

Theorem 12. *Let L be a link in $L(p,q)$ described by the band diagram B. Then*

$$\langle \widehat{B} \rangle^p \equiv \langle \widehat{B^p \Delta_t^{2q}} \rangle \bmod I, \tag{1}$$

where I is the ideal generated by p, $\delta^{p-1}-1$ and the family $\{\langle \widehat{Id_{t-2i}} \rangle^p - \langle \widehat{\Delta_{t-2i}^{2q}} \rangle \}_{i=0,\ldots,\lfloor (t-1)/2 \rfloor}$.

Notice that, if $\delta = (-A^2 - A^{-2})$, then $\langle \widehat{Id_{t-2i}} \rangle^p = \delta^{p(t-2i-1)}$.

Proof. The proof is analogous to the proof of the main theorem of [C]. By modifying the definition of the function f and by verifying that it satisfies the same properties of the original one, we get our statement. $\square$

Example 13. Considering the two links L_A and L_B in $L(4,1)$ of Example 10, we can verify Formula 1. The lift of these two links is the Hopf link, that has Kauffman bracket equal to $-A^4 - A^{-4}$. Since $t = 2$, the ideal I is generated by p, $\delta^3 - 1$ and $\{\langle \widehat{Id_{2-2i}} \rangle^4 - \langle \widehat{\Delta_{2-2i}^2} \rangle \}_{i=0}$, that is to say, p, $-A^6 + A^2 - 1 + A^{-2} - A^{-6}$ and $\langle \widehat{Id_2} \rangle^4 - \langle \widehat{\Delta_2^2} \rangle = \delta^4 - (-A^4 - A^{-4}) = A^8 + 5A^4 + 6 + 5A^{-4} + A^{-8}$. A Groebner basis of I is given by $\{4, A^2 + 1 + A^{-2}\}$.

The closure in $\mathbf{S}^3$ of the band diagram of L_A is the trivial knot, with $\langle L_A \rangle = -A^{-3}$, while the same operation on the band diagram of L_B produces $\langle L_B \rangle = (-A^2 - A^{-2})$.

For the knot L_A, Formula 1 turns into

$$(-A^3)^4 \equiv (-A^4 - A^{-4}) \bmod I.$$

For the link L_B, Formula 1 turns into

$$(-A^2 - A^{-2})^4 = (A^8 + 4A^4 + 6 + 4A^{-4} + A^{-8}) \equiv (-A^4 - A^{-4}) \bmod I.$$

References

[BM]   D. Buck, M. Mauricio, *Connect sum of lens spaces surgeries: application to Hin recombination*, Math. Proc. Cambridge Philos. Soc. **150** (2011), 505–525.

[CMM]   A. Cattabriga, E. Manfredi, M. Mulazzani, *On knots and links in lens spaces*, Topology Appl. **160** (2013), 430–442.

[C]   N. Chbili, *The Jones polynomials of freely periodic knots*, J. Knot Theory Ramifications **9** (2000), 885–891.

[Ch4]   N. Chbili, *A new criterion for knots with free periods*, Ann. Fac. Sci. Toulouse Math. **12** (2003), 465–477.

[DL]   I. Diamantis, S. Lambropoulou, *Braid equivalence in 3-manifolds with rational surgery description*, arXiv:1311.2465 [math.GT] (2013).

[D]   Y. V. Drobotukhina, *An analogue of the Jones polynomial for links in $\mathbb{R}P^3$ and a generalization of the Kauffman-Murasugi theorem*, Leningrad Math. J. **2** (1991), 613–630.

[Ga]   B. Gabrovšek, *Classification of knots in lens spaces*, Ph.D. thesis, University of Ljubljana, Slovenia, 2013.

[GM]   B. Gabrovšek, M. Mroczkowski, *Knots in the solid torus up to 6 crossings*, J. Knot Theory Ramifications **21** (2012), 1250106, 43 pp.

[HP]   J. Hoste, J. H. Przytycki, *The $(2, \infty)$-skein module of lens spaces; a generalization of the Jones polynomial*, J. Knot Theory Ramifications **2** (1993), 321–333.

[M1]   E. Manfredi, *Knots and links in lens spaces*, Ph.D. Thesis, University of Bologna, 2014.

[M2]   E. Manfredi, *Lift in the 3-sphere of knots and links in lens spaces*, J. Knot Theory Ramifications **23** (2014), 1450022, 21 pp.

[P] J. H. Przytycki, *Skein modules of 3-manifolds*, Bull. Polish Acad. Sci. Math. **39** (1991), 91–100.

[S] S. Stevan, *Torus Knots in Lens Spaces & Topological Strings*, to appear on Ann. Henri Poincaré.

[T] V. G. Turaev, *The Conway and Kauffman modules of a solid torus*, J. Soviet Math. **52** (1990), 2799–2805.

BOŠTJAN GABROVŠEK, FME, University of Ljubljana, SLOVENIA. E-mail: bostjan.gabrovsek@fs.uni-lj.si

ENRICO MANFREDI, Department of Mathematics, University of Bologna, ITALY. E-mail: enrico.manfredi3@unibo.it